Electronic Supplementary Material (ESI) for Dalton Transactions.

Azamacrocycles and tertiary amines can be used to form size tuneable hollow structures or monodisperse oxide nanoparticles depending on the 'M' source.

Graham E. Tilburey,[1] Toby J. Blundell,[2] Stephen P. Argent[3] and Carole C. Perry[1*]

[1] Biomolecular and Materials Interface Research Group, Interdisciplinary Biomedical Research Centre, Nottingham Trent University, Clifton Lane, Nottingham NG11 8NS

[2] Department of Chemistry and Forensics, Nottingham Trent University, Clifton Lane, Nottingham NG11 8NS

[3] School of Chemistry, University of Nottingham, University Park, Nottingham NG7 2RD

In honour of the 60th birthday celebrations of Professor Annie Powell.

Contents

S1: Additives investigated (macrocycles and amines)

S2: Yields for syntheses performed at different pH values and Si:N ratios

S3– Silicon catecholate: cyclam at a Si:N ratio of 10:1. (SEM images)

S4: SEM and EDXA data for typical samples isolated from a reaction between potassium silicon catecholate with cyclam at a 10:1 Si:N molar ratio performed at pH 6.85 and isolated after 1 hour.

S5: Estimation of chemical composition from TGA and CHN analysis for complex formed between potassium silicon catecholate and cyclam.

S6: Characterisation of tetragonal prisms prepared at an Si:N ratio of 1:10 and isolated at either 5 minutes or 1 hour. (TGA, powder XRD, SEM/ EDX)

S7: Crystal structure data for complex formed between potassium silicon catecholate and cyclam. CCDC 1916071

S8: The formation and characterisation of tetragonal prisms using dipotassium tris(1,2-benzenediolato-*O,O'*)germanate- synthesis and characterisation

S9: Reaction between potassium silicon catecholate and diamines MEDAE, MEDAB and MEDAH- further characterisation

S10: Comparison of experimental powder x-ray diffraction patterns for (a) Sicat:cyclam; (c) Gecat:cyclam and (d) Sicat:MEDAE complexes together with the powder pattern generated from the single crystal data for Sicat:cyclam (b).

S1: Additives investigated

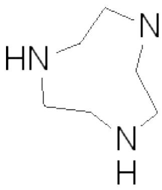

3NC

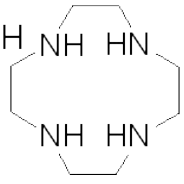

4N2

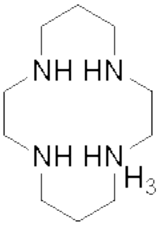

cyclam

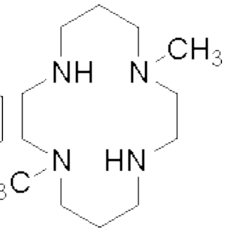

2MC

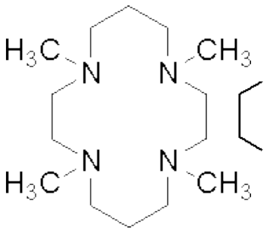

4MC

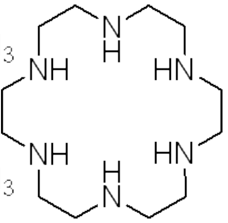

6NC

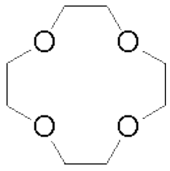

12C4

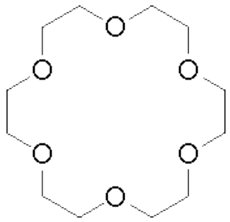

18C6

Macrocyclic compounds:

From left to right, top to bottom: 1,4,7-triazacyclononane (3NC), 1,4,7,10-tetraazacyclododecane (4N2), 1,4,8,11-tetraazacyclodecane (cyclam), 1,8 dimethyl 1,4,8,11-tetraazacyclodecane (2MC), 1,4,8,11-tetra methyl 1,4,8,11 tetraazacyclodecane (4MC), 1,4,7,10,13,16-hexaazacyclooctadecane (6NC). 12-crown-4 (12C4) and 18-crown-6 (18C6).

Amines:

Name	Amine architecture
N,N′-Bis(3-aminopropyl)-1,3-propanediamine	1/2
Bis(3-aminopropyl)amine	1/2
N,N′-Dimethyl-1,6-hexanediamine	2
Tris(dimethylamino)methane	3
1,1,4,7,10,10-Hexamethyltriethylenetetramine	3
3,3′-Iminobis(N,N-dimethylpropylamine)	3
1,3-Diamino-2-hydroxypropane-N,N,N',N'-tetraacetic acid	3
3-(Dimethylamino)-1-propylamine	3
N,N,N′,N′-Tetramethyldiaminomethane	3
N,N,N′,N′-Tetramethylethylenediamine	3
N,N,N′,N′-Tetramethyl-1,4-butanediamine	3
N,N,N′,N′-Tetramethyl-1,6-hexanediamine	3
N,N,N′,N″,N″-Pentamethyldiethylenetriamine	3/1
N,N,N′-Trimethyl-1,3-propanediamine	3/1
N,N,N′-Trimethylethylenediamine	3/2

1 = primary, 2 = secondary, 3 = tertiary.

S2: Yields for syntheses performed at different pH values and Si:N ratios.

Molecular formula	$C_{28}N_4O_8H_{48}Si$ (assuming 2 molecules of water per mole of complex)
Molecular weight of new complex =	588.33
No µmoles of cyclam =	7.4

a)

pH	Mass of complex /mg	No. moles of complex /µM	Yield /%
6.95	3.9	6.63	89.6
7.182	3.7	6.29	85.0
7.374	3.5	5.95	80.4
7.506	3.2	5.44	73.5
7.64	3.3	5.61	75.8
7.768	4	6.80	91.9
7.922	2.7	4.59	62.0
8.094	4.2	7.14	96.5
8.356	3.3	5.61	75.8
8.715	4.3	7.31	98.8
9.650	4.3	7.31	98.8

b)

Concentration	Mass of complex /mg	No. moles cyclam /µM	No. moles of complex /µM	Yield /%
10:3	10.6	22.5	18.01709925	80.1
10:5	19.8	37.4	33.65458161	90.0
10:7	27.1	52.4	46.06258392	87.9
10:10	32.2	74.9	54.73118828	73.1

S3– Silicon catecholate: cyclam at a Si:N ratio of 10:1.

SEM micrographs of material formed from the reaction of potassium silicon catecholate with cyclam at a 10:1 Si:N molar ratio and isolated after; a) 25 s, b) 5 minutes, c) 60 minutes, d) 132 minutes, e) 346 minutes and f) 24 h.

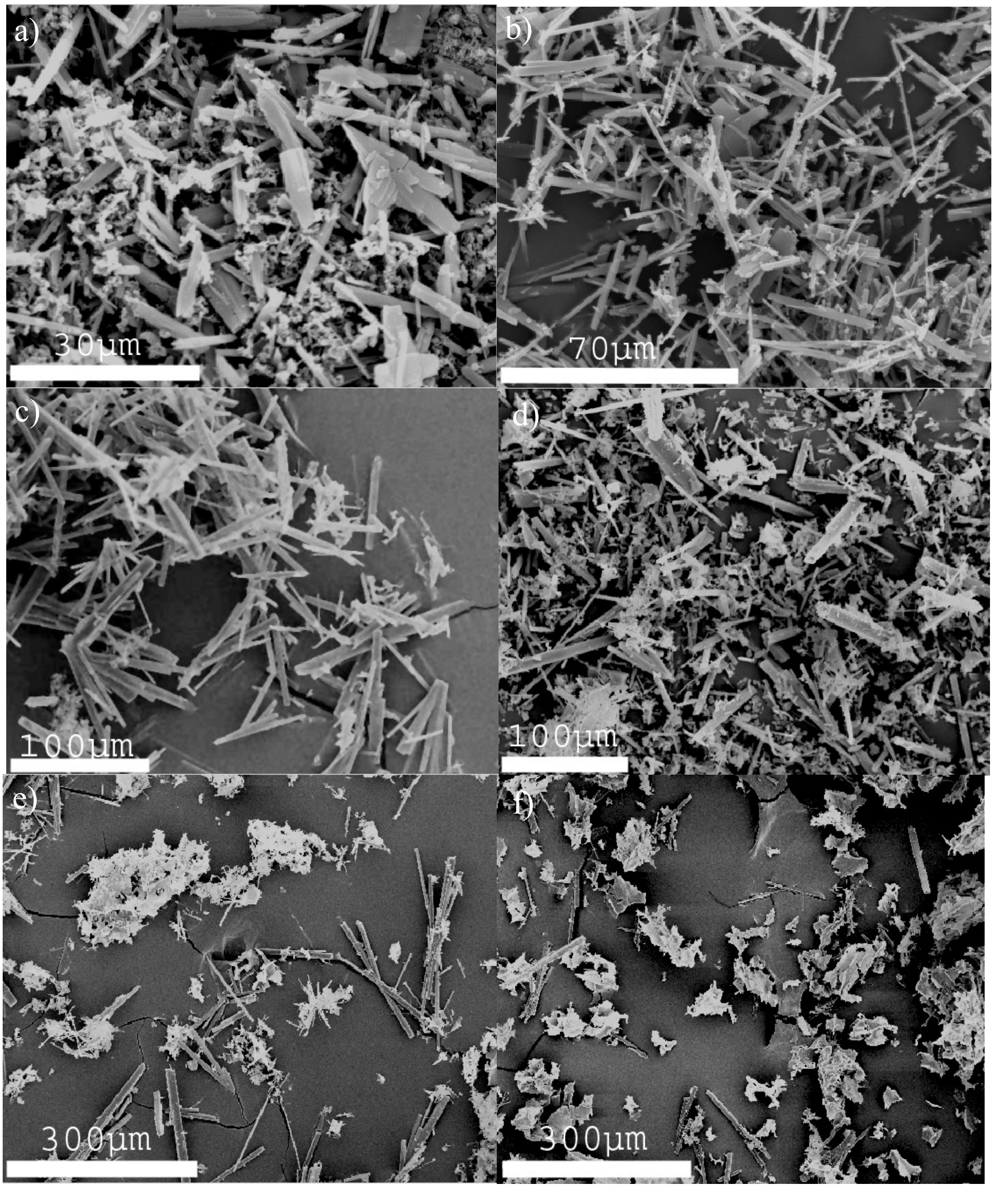

By choosing the time of sample collection one can either selectively isolate essentially only tetragonal prismatic tubes or mixtures of the tubes and silica which forms later in the reaction when cyclam levels have been depleted.

S4: SEM and EDXA data for typical samples isolated from a reaction between potassium silicon catecholate with cyclam at a 10:1 Si:N molar ratio performed at pH 6.85 and isolated after 1 hour.

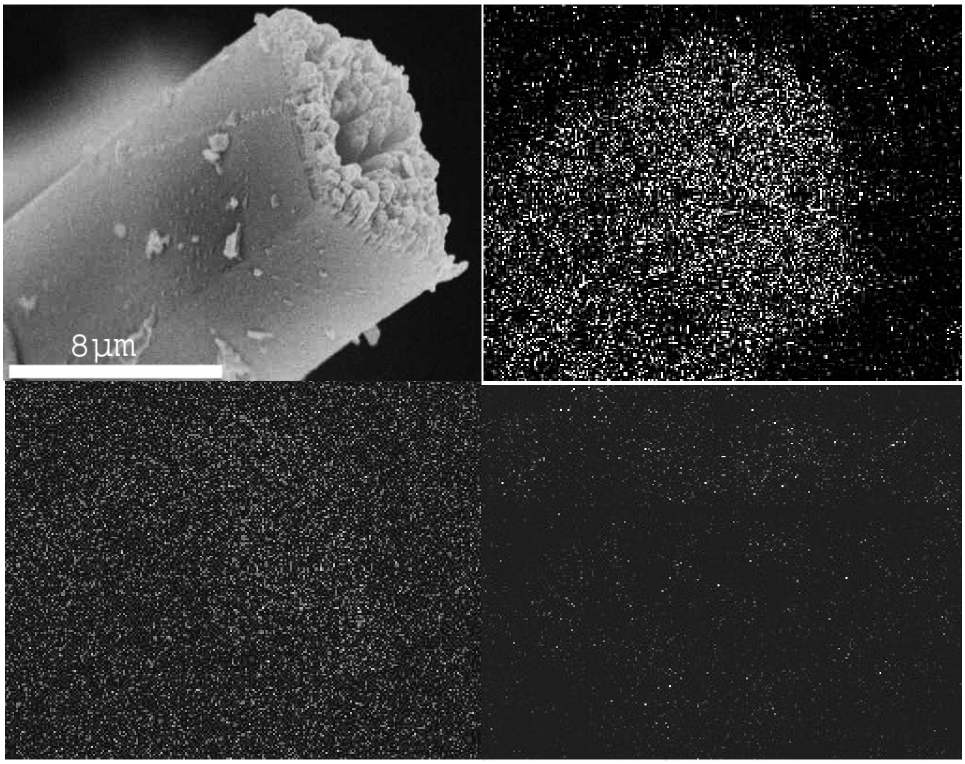

Top left) tetragonal prism used for EDXA analysis, top right) EDXA mapping for silicon, bottom left) oxygen and bottom right) potassium.

Data show that the hollow tubes contain both the silicon catecholate and cyclam but NO potassium.

S5: Estimation of chemical composition from TGA and CHN analysis for complex formed between potassium silicon catecholate and cyclam.

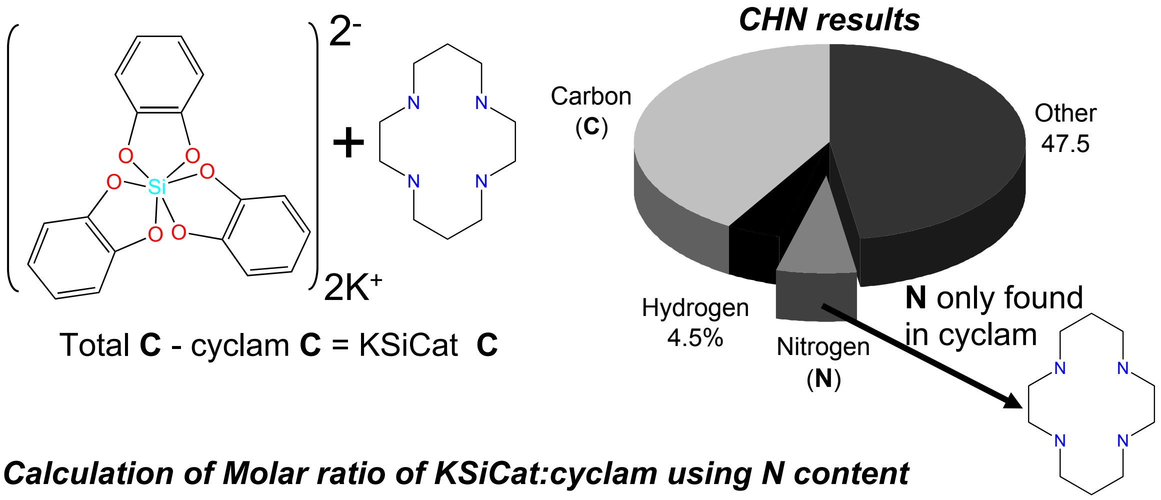

Calculation of Molar ratio of KSiCat:cyclam using N content

Cyclam	% in Molecule	% in Unknown
4N	0.280	**6.7**
10C	0.600	14.4
24H	0.121	2.9
	N Mole %	93.8

KSiCat	% in Molecule	% in Unknown
18C	61.4	**28.8**
6O	27.2	12.8
12H	3.4	3.6
Si	8.0	3.7
	Si Mole %	104.8

Molar ratio of ~1:1 in crystalline material

The molecular composition of the crystalline material was investigated by performing CHN analysis. The composition was found to be 41.3% Carbon, 6.7% Nitrogen and 4.5% Hydrogen. These results can be used to calculate the crystal composition from the amount of nitrogen found in the sample, which can be attributed solely to cyclam. From this percentage the amount of carbon associated with the cyclam molecule can be calculated, thus the remaining carbon can be attributed to SiCat. Conversion of the % mass of nitrogen in cyclam and % silicon to mole % allows us to show the molecular composition of the crystal is 1:1 with respect to cyclam and SiCat. EDS analysis suggests that the potassium associated with SiCat has been removed from the structure, which suggests cyclam has two of the amine residues in its structure protonated to balance the charge on the SiCat molecule.

S6: Characterisation of tetragonal prisms prepared at an Si:N ratio of 1:10 and isolated at either 5 minutes or 1 hour.

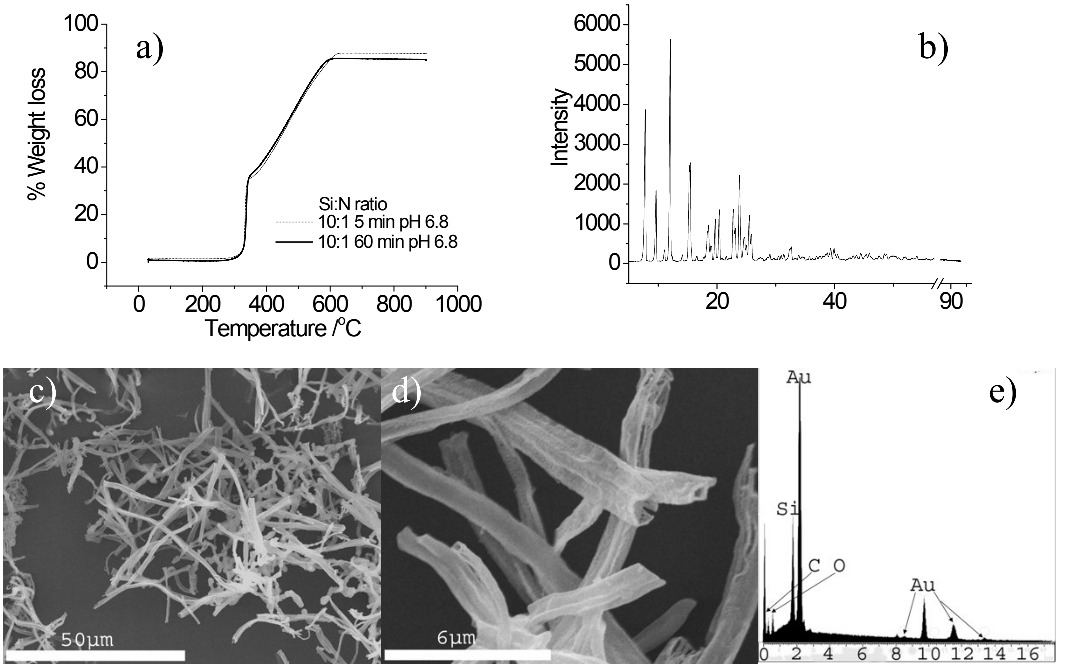

Thermal gravimetric analysis of tetragonal prisms prepared at an Si:N ratio of 1:10 isolated after 5 and 60 minutes, b) Powder XRD of tetragonal prisms formed at pH 8.2 with an Si:N ratio of 10:1, c and d) SEM micrographs show the heat-treated material and the partial retention of tetragonal prism structure, e) EDX spectra of heat-treated tetragonal prisms.

Note, the tube-like objects form very early in the reaction and do not change their structure with time (TGA traces do not differ significantly for the samples isolated at either 5 or 60 minutes after the start of the reaction). The x-ray powder diffraction pattern and its calculated equivalent (from single crystal x-ray) are shown in SI10 for ease of comparison.

S7: Crystal structure data for complex formed between potassium silicon catecholate and cyclam. CCDC 1916071

Crystal data and structure refinement for shelxt.

Identification code	SATSTC
Empirical formula	$C_{28}H_{40}N_4O_7Si$
Formula weight	572.73
Temperature/K	100
Crystal system	triclinic
Space group	P-1
a/Å	9.88046(17)
b/Å	11.9013(2)
c/Å	12.18161(18)
α/°	77.2668(15)
β/°	81.0651(14)
γ/°	86.7154(16)
Volume/Å^3	1379.86(3)
Z	2
ρ_{calc}g/cm^3	1.378
μ/mm^{-1}	0.134
F(000)	612.0
Crystal size/mm^3	0.1 × 0.01 × 0.01
Radiation	Synchrotron (λ = 0.6889)
2Θ range for data collection/°	3.358 to 71.95
Index ranges	$-16 \leq h \leq 16$, $-20 \leq k \leq 20$, $-19 \leq l \leq 20$
Reflections collected	29477
Independent reflections	12427 [R_{int} = 0.0541, R_{sigma} = 0.0804]
Data/restraints/parameters	12427/0/388
Goodness-of-fit on F^2	1.068
Final R indexes [I>=2σ (I)]	R_1 = 0.0619, wR_2 = 0.1843
Final R indexes [all data]	R_1 = 0.0996, wR_2 = 0.2022
Largest diff. peak/hole / e Å^{-3}	0.61/-1.00

```
Hydrogen bonds with  H..A < r(A) + 2.000 Angstroms  and  <DHA > 110 deg.
 Appropriate HTAB instructions appended to .res file for future use.
 D-H            d(D-H)  d(H..A)  <DHA   d(D..A)   A
 N1-H1A           0.818   2.555  121.41   3.062   O3
 N1-H1A           0.818   1.946  169.76   2.755   O5
 N1-H1B           0.872   2.125  133.95   2.802   N2
 N2-H2          0.961   2.029  172.40   2.984   O1
 N3-H3A           1.021   2.441  122.51   3.111   O2 [ x-1, y, z ]
 N3-H3A           1.021   1.778  162.21   2.768   O4 [ x-1, y, z ]
 N3-H3B           0.863   2.144  135.69   2.827   N4
```

N4-H4	0.917	2.095	171.19	3.004	O6 [x-1, y, z]
C3-H3	0.950	2.556	128.91	3.238	O7 [-x+2, -y+1, -z+2]
C19-H19A	0.990	2.400	171.70	3.382	O7 [x-1, y, z]

Bond Lengths for shelxt.

Atom	Atom	Length/Å	Atom	Atom	Length/Å
Si1	O1	1.7927(11)	C10	C11	1.403(2)
Si1	O2	1.7983(11)	C11	C12	1.3820(19)
Si1	O3	1.7775(11)	C13	C14	1.3837(19)
Si1	O4	1.7916(10)	C13	C18	1.404(2)
Si1	O5	1.7966(10)	C14	C15	1.405(2)
Si1	O6	1.7847(11)	C15	C16	1.380(2)
O1	C1	1.3445(18)	C16	C17	1.406(2)
O2	C6	1.3649(19)	C17	C18	1.382(2)
O3	C7	1.3451(16)	N1	C19	1.4983(19)
O4	C12	1.3530(17)	N1	C28	1.4851(19)
O5	C13	1.3571(18)	N2	C21	1.477(2)
O6	C18	1.3565(17)	N2	C22	1.469(2)
C1	C2	1.391(2)	N3	C23	1.493(2)
C1	C6	1.397(2)	N3	C24	1.4933(19)
C2	C3	1.402(2)	N4	C26	1.472(2)
C3	C4	1.382(3)	N4	C27	1.4670(18)
C4	C5	1.402(2)	C19	C20	1.519(2)
C5	C6	1.383(2)	C20	C21	1.529(2)
C7	C8	1.383(2)	C22	C23	1.526(2)
C7	C12	1.4143(19)	C24	C25	1.523(2)
C8	C9	1.401(2)	C25	C26	1.529(2)
C9	C10	1.390(2)	C27	C28	1.521(2)

Bond Angles for shelxt.

Atom	Atom	Atom	Angle/°	Atom	Atom	Atom	Angle/°

O1	Si1	O2	88.21(5)	C8	C7	C12	119.71(12)
O1	Si1	O5	88.67(5)	C7	C8	C9	119.14(14)
O3	Si1	O1	88.16(5)	C10	C9	C8	120.96(14)
O3	Si1	O2	174.94(5)	C9	C10	C11	120.18(13)
O3	Si1	O4	88.89(5)	C12	C11	C10	118.74(13)
O3	Si1	O5	89.29(5)	O4	C12	C7	113.47(11)
O3	Si1	O6	94.24(5)	O4	C12	C11	125.29(13)
O4	Si1	O1	93.92(5)	C11	C12	C7	121.22(13)
O4	Si1	O2	87.84(5)	O5	C13	C14	125.08(14)
O4	Si1	O5	176.78(5)	O5	C13	C18	113.57(12)
O5	Si1	O2	94.15(5)	C14	C13	C18	121.35(14)
O6	Si1	O1	176.06(5)	C13	C14	C15	118.12(14)
O6	Si1	O2	89.58(5)	C16	C15	C14	120.65(14)
O6	Si1	O4	89.25(5)	C15	C16	C17	121.11(15)
O6	Si1	O5	88.23(5)	C18	C17	C16	118.41(15)
C1	O1	Si1	112.06(10)	O6	C18	C13	113.73(13)
C6	O2	Si1	111.45(10)	O6	C18	C17	125.92(14)
C7	O3	Si1	112.03(9)	C17	C18	C13	120.34(13)
C12	O4	Si1	111.53(8)	C28	N1	C19	115.66(11)
C13	O5	Si1	111.89(9)	C22	N2	C21	113.90(12)
C18	O6	Si1	112.18(9)	C24	N3	C23	115.44(12)
O1	C1	C2	125.14(15)	C27	N4	C26	113.18(12)
O1	C1	C6	114.35(13)	N1	C19	C20	110.07(12)
C2	C1	C6	120.52(14)	C19	C20	C21	113.53(13)
C1	C2	C3	118.70(16)	N2	C21	C20	111.73(13)
C4	C3	C2	120.49(15)	N2	C22	C23	111.87(12)
C3	C4	C5	120.79(15)	N3	C23	C22	111.94(12)
C6	C5	C4	118.69(16)	N3	C24	C25	110.83(12)
O2	C6	C1	113.66(13)	C24	C25	C26	114.46(13)
O2	C6	C5	125.55(15)	N4	C26	C25	111.02(12)
C5	C6	C1	120.80(15)	N4	C27	C28	111.48(12)
O3	C7	C8	126.32(13)	N1	C28	C27	112.10(12)
O3	C7	C12	113.95(12)				

S8: The formation and characterisation of tetragonal prisms using dipotassium tris(1,2-benzenediolato-*O,O'*)germanate

Base was added to the KGeCat solution to provide a range of pH values compatible with the different protonation states of cyclam. Hollow tetragonal prisms (ca. 30 x 3 microns- smaller than for Si) were formed over a wide pH range (6.7-11.4) whose x-ray powder diffraction pattern was very similar to that generated for the Si based materials.

Summary of results obtained when using KGeCat and cyclam at a Ge:N ratio of 10:1 to form tetragonal prisms.

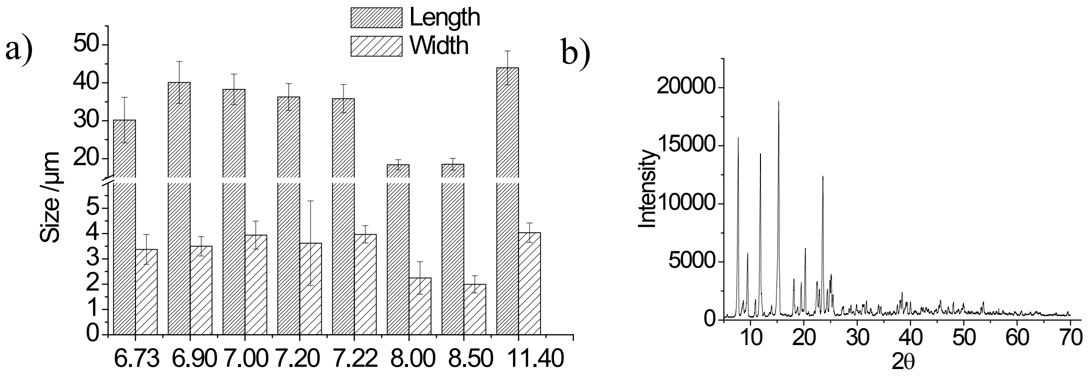

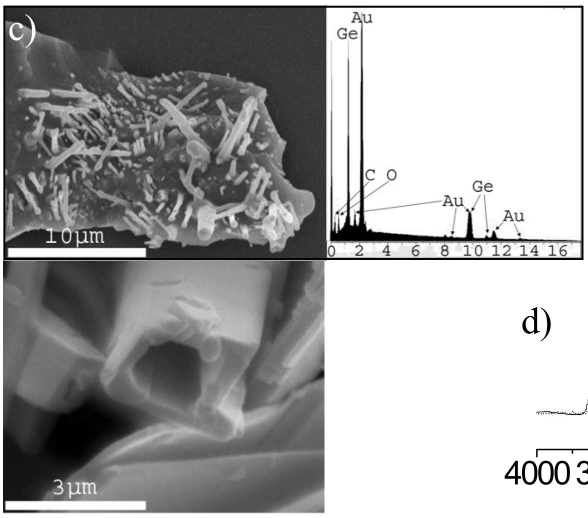

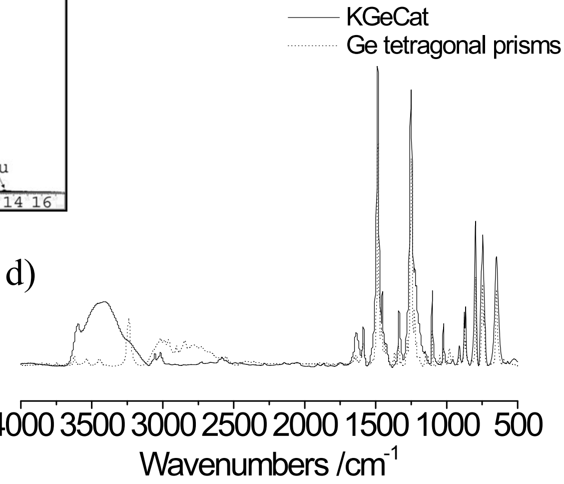

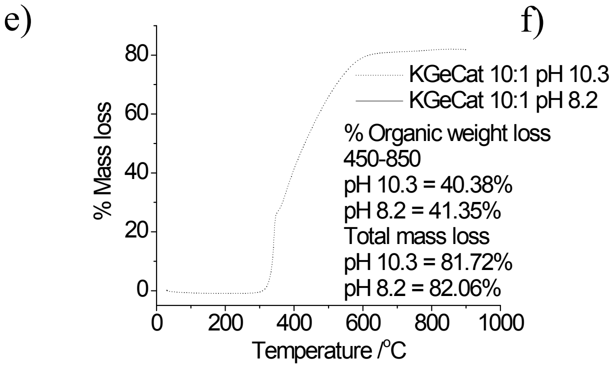

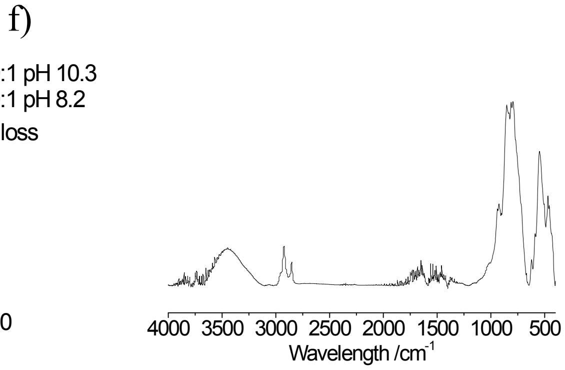

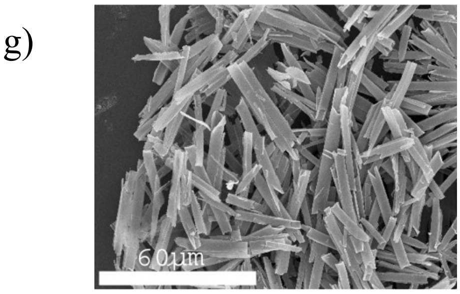

a) Effect of pH on the sizes of Ge tetragonal prisms formed b) Powder XRD of the tetragonal prisms formed from KGeCat at pH 10.3. - c) SEM micrographs; Top left: thermally treated KGeCat tetragonal prisms, top right; EDXA spectra confirming the material is germanium based. Bottom: germanium tetragonal prism. d) FTIR of Ge tetragonal prism and KGeCat e) TGA at pH 8.2 and 10.3. f) FTIR of thermally treated Ge tetragonal prisms g-k) effect of concentration on Ge tetragonal prism formation; 10:1.

S9: Reaction between potassium silicon catecholate and diamines MEDAE, MEDAB and MEDAH

Reaction between potassium silicon catecholate and MEDAE at a molar ratio Si:N of 1:1. Hexagonal rods formed over a wide pH, see figure below with the structures gradually changing from hollow hexagonal needles through to rods as the pH of the reaction increased. Materials were characterised by SEM, EDXA, powder XRD, TGA and FTIR.

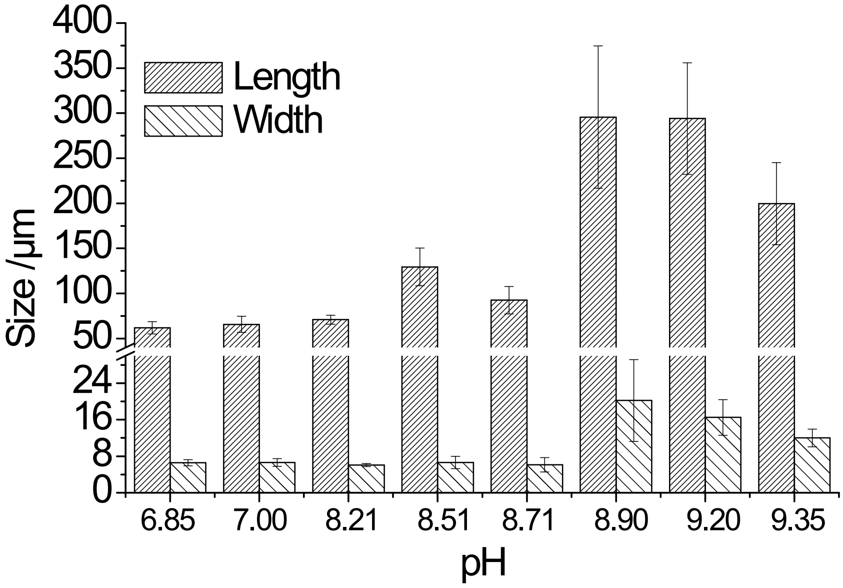

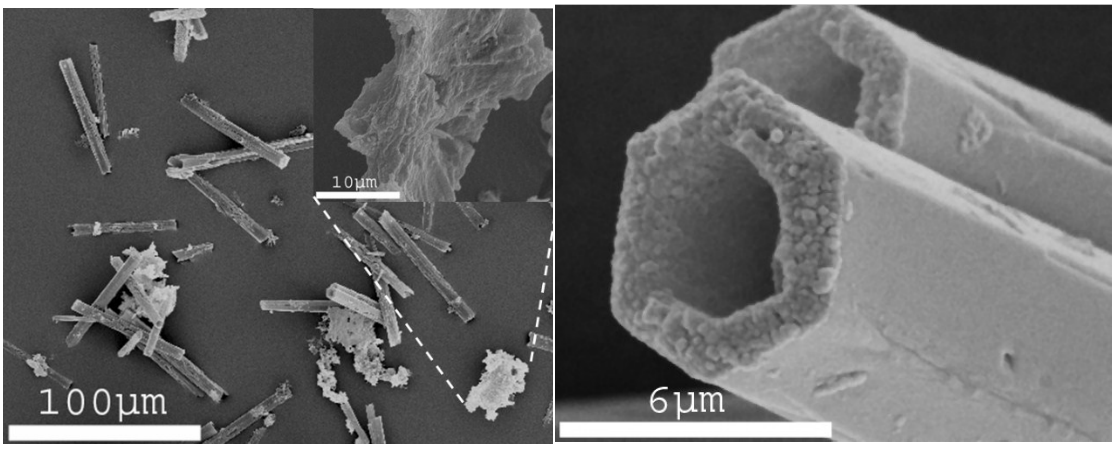

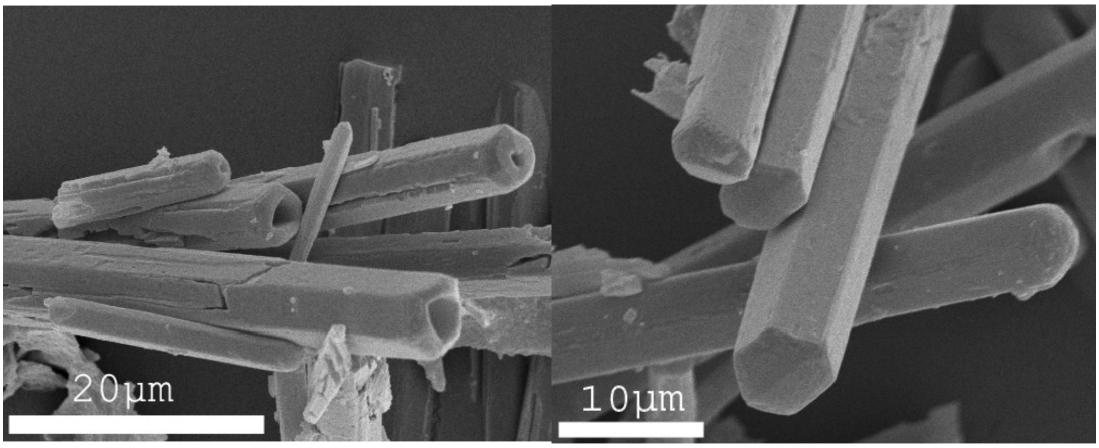

SEM micrographs show the structures precipitated from solution at; top row pH 6.85, bottom left pH 8.21 and bottom right) 8.51.

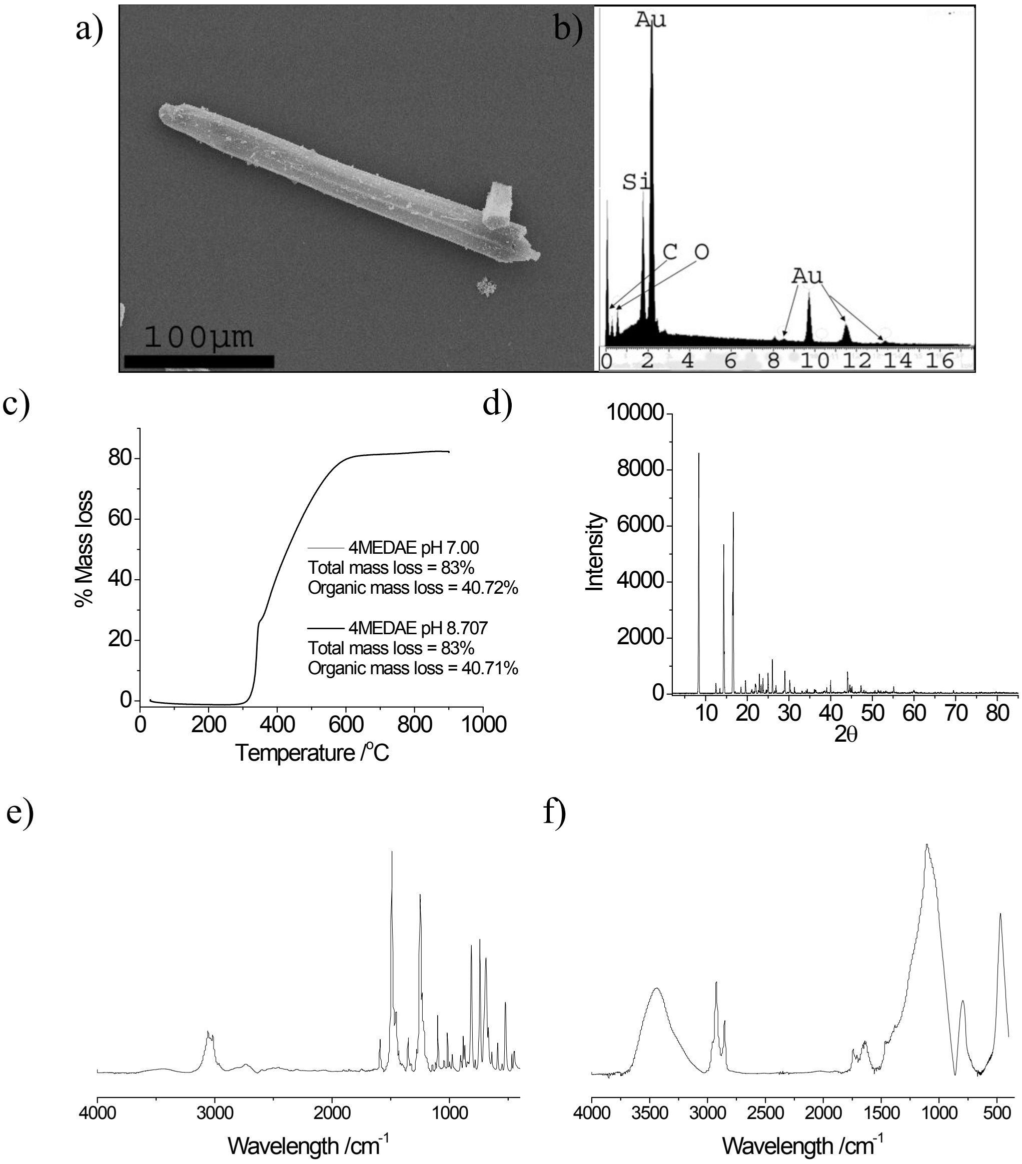

a) SEM micrograph of the material remaining after TGA showing retention of the rod morphology accompanied by b) the EDXA spectra showing the material is silicon based. c) TGA of hexagonal prisms formed at pH 8.51 Si:N ratio1:1. d) Powder XRD of hexagonal rods prior to TGA. e) and f) FTIR spectra before and after thermal treatment.

Following thermal treatment there was a remarkable retention of the rod-like morphology despite being just 13 % silica. The material precipitated at pH 8.51 was investigated using FTIR before and after thermal gravimetric analysis. Figure e above shows the FTIR spectra of the material produced at pH 8.51 prior to thermal analysis indicating the presence of the SiCat, where characteristic peaks at *ca*. 3060 and 3015 cm^{-1} and a sharp peak at 1100 cm^{-1} indicate aromatic C-H bonds and Si-O in an octahedral conformation respectively. Interestingly, as seen with the KGeCat tetragonal prisms Figure f above shows some organic material remains in the thermally treated tetragonal prisms indicated firstly by the CH_3 peaks at 2924 and 2854 cm^{-1} and secondly the peaks at 1743 and 1637cm^{-1} which one would hypothesise to arise from N-H bonds.

4MEDAB was investigated, where B (butane) relates to the number of carbon atoms separating the tertiary amine groups, increased from 2 to 4. Unsurprisingly this molecule also forms a complex with KSiCat. The figure below, as well as that shown in Fig. 7 in the main text of the paper, shows the morphology of the material precipitated from solution after 60 minutes, where a hexagonal plate morphology can be prepared at pH 8.25 at a Si:N ratio of 1:1. It was found while trying to study a complete pH range that the precipitates formed at pH 8.25-8.9 could not be isolated as the material dissolved when it was washed with dd water to ensure the precipitate was free of KCl. This indicated that either the precipitate was composed of KCl or the complex formed between KSiCat and 4MEDAB was now highly unstable to even mildly acid conditions exhibited by dd water *ca.* pH 5. Analysis by FTIR confirmed the presence of both species.

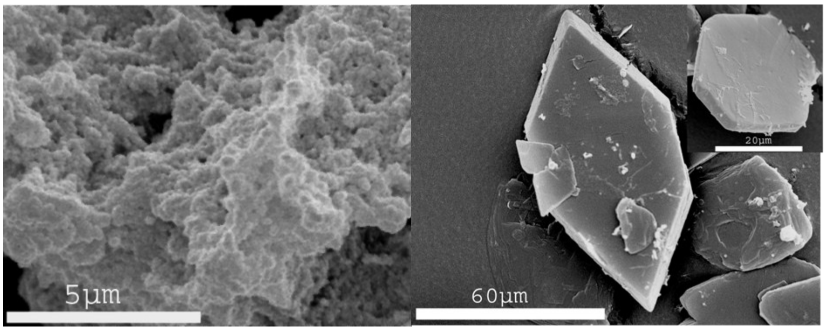

Morphology of precipitate made using 4MEDAB at a Si:N ratio of 1:1 isolated after 1 h. LHS pH 6.8, RHS pH 8.25, with insert showing other hexagonal structures observed as shown in Fig. 7.

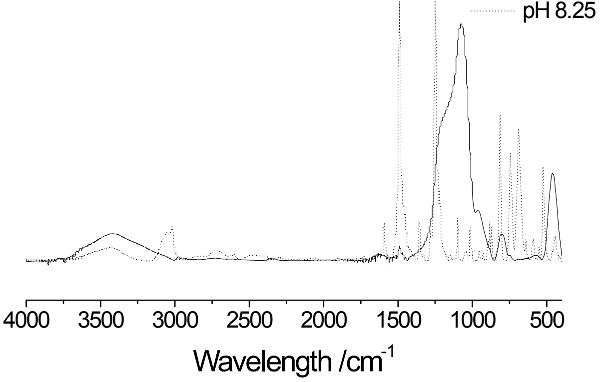

FTIR spectra of precipitated material using 4MEDAB at Si:N 1:1 at pH 6.8 silica is precipitated. At pH 8.25 SiCat:amine complex is precipitated.

A further increase of the spacing of the amine groups to 6 carbon atoms lead to a range of structures, depicted below whose composition could be inferred from FTIR data.

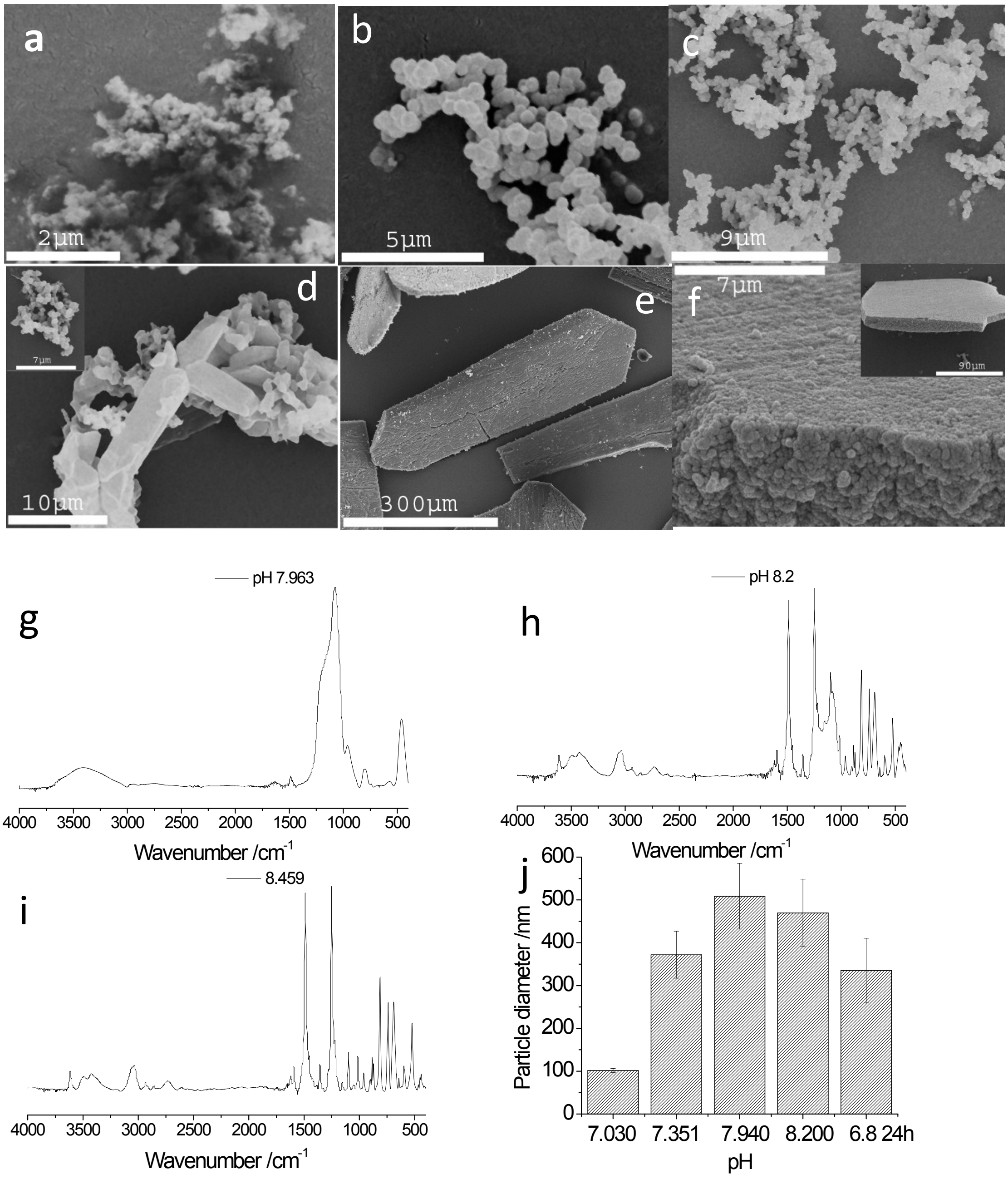

Morphology of the precipitate isolated after 60 minutes using 4MEDAH at an Si:N ratio of 1:1 after 1 h at pH a) 7.030 b) 7.351 insert shows this system is bimodal containing amorphous silica with a spherical morphology and larger plate-like structures c) 7.963 d) 8.2 and e) 8.459 and f) 6.8 after 24 h, insert shows macroscopic structure of the spherical particles assembled into a macroscopic sheet. g-i) FTIR spectra of material isolated at pH 7.963, 8.2 and 8.459. j) characterisation of the silica spheres precipitated at pH 7-8.2 after 60 minutes and at pH 6.8 after 24 h.

The FTIR spectra shown above show the transition of the precipitated material from silica, characterised by the Si-O-Si peak at 1100 cm^{-1} through to a silicon catecholate:amine complex as the pH of the reaction medium was increased. Specifically, the material isolated at pH 8.2 as shown in the SEM micrograph shows a bimodal system thought to comprise silica spheres and larger plate-like structures though to be complexed SiCat. The FTIR spectrum shown in Figure h seems to confirm this hypothesis as it shows characteristic peaks of SiCat at 1495 and 1248 cm^{-1} attributable to a substituted aromatic ring and the aryl =C-0 respectively. Importantly the confirmation that this is a bimodal system comes from the broad band centring at 1100 cm^{-1} which is sharp at the top of the peak but broad at the base. This indicates some complexed SiCat where the Si-O is probably in a single octahedrally coordinated environment and the broadening at the base is cause by the presence of amorphous silica. The FTIR spectra shown in Figure i is characteristic of complexed SiCat and when compared to the material isolated at pH 8.2 a sharp peak at 1100 cm^{-1} and no broadening at the base indicating that the conditions now favour SiCat complexation and not silica formation.

S10: Comparison of experimental powder x-ray diffraction patterns for (a) Sicat:cyclam; (c) Gecat:cyclam and (d) Sicat:MEDAE complexes together with the powder pattern generated from the single crystal data for Sicat:cyclam (b).

Diffractograms are presented together to make it easier to compare their similarities and differences for materials where it was possible to obtain a single crystal x-ray diffraction pattern (a) and others where this has not been possible to date (c (Ge catecholate cyclam complex) and d (Si catecholate- MEDAE complex)). Further, the calculated powder x-ray diffraction pattern for the silicon catecholate: cyclam complex is provided in (b). Note, although measured diffractograms for the Si and Ge species are very similar there are differences in intensities between the measured and simulated data for the Si species. This is probably due to preferential orientation of the rod-like crystals though to date we have no further data to support this supposition.